Downregulation of miR-499a-5p Predicts a Poor Prognosis of Patients With Non-Small Cell Lung Cancer and Restrains the Tumorigenesis by Targeting Fibroblast Growth Factor 9

Lihong Zhao, MM[1] ⬤, Ping Jiang, MM[1], Hong Zheng, MM[1], Panfeng Chen, MM[1], and Min Yang, MM[1]

Abstract

The aberrant expression of microRNA is an important regulator in the tumorigenesis of non-small cell lung cancer. In this study, we found that miR-499a-5p was notably downregulated in non-small cell lung cancer tissues and cell lines. Decreased miR-499a-5p expression was associated with larger tumor size and higher TNM stage. Non-small cell lung cancer patients with low expression of miR-499a-5p exhibited a worse overall survival rate compared with those patients with high expression of miR-499a-5p. Ectopic expression of miR-499a-5p significantly suppressed non-small cell lung cancer cell proliferation and colony formation, and hampered cell cycle at G0/G1 phase *in vitro*. Conversely, knockdown of miR-499a-5p promoted non-small cell lung cancer cell proliferation and colony formation, and induced cell cycle at S phase. Furthermore, *in vivo* experiments revealed that over-expression of miR-499a-5p inhibited the tumor formation in a nude mouse xenograft model. Mechanistic studies showed that fibroblast growth factor 9 was a direct target gene of miR-499a-5p. miR-499a-5p directly bound to fibroblast growth factor 9 mRNA 3'-UTR, therefore led to the reduction in fibroblast growth factor 9 protein expression. Finally, rescue experiments confirmed that silencing of fibroblast growth factor 9 partially reversed the phenotypes of miR-499a-5p knockdown on non-small cell lung cancer cell proliferation. In conclusion, our study demonstrates that downregulation of miR-499a-5p predicts a worse prognosis of patients with non-small cell lung cancer and restrains the tumorigenesis by targeting fibroblast growth factor 9. These findings may provide valuable clues for the future development of therapeutic strategies against this cancer.

Introduction

Lung cancer is one of the most frequently diagnosed malignancies and the leading cause of cancer-associated death globally, approximately $80 \sim 85\%$ of lung cancer is classified pathologically as non-small cell lung cancer (NSCLC).[1,2] Compared to other subtypes of lung cancer, the overall survival of NSCLC remains unsatisfactory, with a 5-year survival rate of only $10 \sim 15\%$.[3,4] Despite considerable advances in diagnosis, surgery, chemotherapy, and radiotherapy, the treatment of NSCLC remains a big challenge due to a lack of specific and effective therapeutic targets. Therefore, there is a great need for the development of strategies for improved diagnosis and therapy for NSCLC treatment that are based on the molecular mechanisms underlying the tumorigenesis of NSCLC.

MicroRNA (miRNA) is a class of small endogenous non-coding RNA molecules ($18 \sim 25$ nt in length) found in eukaryote that is responsible for the degradation of mRNA or translation inhibition by binding to 3'-non coding region (3'-UTR) of target genes.[5,6] miRNA regulates the expression of approximately a third of human genes, and affects diverse

[1] Department of Respiratory and Critical Care Medicine, Tianjin First Central Hospital, Tianjin, China

Corresponding Author:
Lihong Zhao, Department of Respiratory and Critical Care Medicine, Tianjin First Central Hospital, No. 24, Fukang Road, Nankai District, Tianjin 300192, China.
Email: zhaolhyzx@163.com

cellular activities, such as cell growth, migration, apoptosis, and differentiation.[7,8] In the past 2 decades, numerous studies have proofed that miRNA play complex and key roles in the development of human cancer.[9] For example, An et al demonstrated that miR-944 inhibits lung cancer tumorigenesis by targeting signal transducer and activator of transcription 1. Hu et al reported that miR-204 inhibits metastasis of lung cancer by targeting sex-determining region Y-box 4.[10] An et al showed that upregulated miR-21 expression promotes the development of lung cancer through inhibition of WW and C2 domain containing 1 and the Hippo signaling pathway.[11] Li et al indicated that miR-1-3p inhibits lung cancer tumorigenesis via targeting protein regulator of cytokinesis 1.[12] Although the dysregulation of miRNA has been shown in lung cancer, the emerging functions of miRNA in the tumorigenesis of NSCLC remain largely unknown.

Previous studies have demonstrated that miRNA profiling can be achieved by mining published gene expression microarray data.[13] Genome-wide miRNA expression profiling has shown that miR-499a-5p is downregulated in lung cancer.[14] However, the roles and mechanisms of miR-499a-5p in NSCLC remain poorly understand. Fibroblast growth factor 9 (FGF9) is a secretory protein belonging to the FGFs family.[15] Previous reports have displayed that FGF9 is a key mediator of tumorigenesis in several human cancers, including NSCLC, hepatocellular carcinoma, and prostate cancer.[16-18] Interestingly, using bioinformatics analysis, we found that the sequences of FGF9 mRNA 3'-UTR could directly bind with miR-499a-5p. Based on this, the aim of our study was designed to investigate the regulatory mechanism between miR-499a-5p and FGF9 on the tumorigenesis of NSCLC. We found that miR-499a-5p was downregulated in NSCLC tissues and cell lines. miR-499a-5p inhibited NSCLC cells proliferation *in vitro* and restrained the tumorigenesis of NSCLC *in vivo*. Furthermore, we identified that FGF9 was a target gene of miR-499a-5p, and silencing of FGF9 partially reversed the phenotypes of miR-499a-5p knockdown on NSCLC cell proliferation. Our findings provided a theoretical basis for the mechanism of miR-499a-5p/FGF9 axis in the tumorigenesis of NSCLC.

Material and Methods

Patients Collection

Paired cancer tissues and matched adjacent normal tissues from 110 NSCLC patients (63 males and 47 females, a median age of 53.8 ± 6.2 years) undergoing pulmonary resection were obtained from Tianjin First Central Hospital (Tianjin, China) between April 2016 and September 2018. All patients recruited in this study were not subjected to preoperative radiotherapy and/or chemotherapy, and were diagnosed by 2 pathologists. All tissues were frozen immediately at liquid nitrogen and used for extraction of RNA. This study was approved by the Ethics Committee of Tianjin First Central Hospital (permit number: TJ201601071), and written informed consent was obtained from all patients prior to enrollment in the present study.

Cell Transfection

Three human NSCLC cell lines (A549, H1299, and PC-9) and a normal bronchial epithelial cell line (BEAS-2B) were purchased from the Cell Bank of the Type Culture Collection of the Chinese Academy of Sciences (Shanghai, China). The cells were cultured in Dulbecco's modified Eagle's medium (Gibco, Carlsbad, CA, USA) supplemented with 10% fetal bovine serum (Gibco, Carlsbad, CA, USA), 100 U/mL penicillin, and 100 μg/mL streptomycin in a humidified atmosphere of 5% CO_2 at 37°C. The cells in the exponential phase of growth were used for cell transfection. The agomiR-499a-5p and corresponding agomiR-NC (#miR40002870-4-5), antagomiR-499a-5p and corresponding antagomiR-NC (#miR30002870-4-5) were constituted by RiboBio Co., Ltd. (Guangzhou, China). The FGF9 siRNA (siFGF9) and corresponding control siRNA (siCtrl) were chemically synthesized by Biomics Biotechnologies (Jiangsu, China). For cell transfection, NSCLC cells were seeded into 6-well plates at 5×10^5 cells/well the day prior to transfection. Then cells were transiently transfected with these oligonucleotides by using Lipofectamine 2000 (Invitrogen, CA, USA), according to the manufacturer's protocol. Then cells were harvested at 48 h after the transfection, and transfection efficiency was determined by detecting miR-499a-5p and FGF9 mRNA expression.

Western Blot Analysis

Proteins were extracted from cells and tissues by using RIPA buffer (Beyotime Biotechnology, China). 30 μg equal amounts of protein lysate were separated on parallel lanes of 10% SDS PAGE gel and then electrotransferred onto a PVDF membrane (Millipore, MA, USA). Following blocking with 5% non-fat milk in phosphate-buffered saline containing Tween 20 buffer (TBS-T) for 1 h at 37°C, the membranes were incubated overnight at 4°C with the following antibodies: FGF9 rabbit polyclonal antibody (#A6374, 1:500 dilution, ABclonal, China), cyclin D1 (CCND1) rabbit monoclonal antibody (#A19038, 1:1500 dilution; ABclonal, China), and GAPDH mouse monoclonal antibody (#AC002, 1:2000 dilution; ABclonal, China). GAPDH was used as a protein loading control. After being washed thrice with TBS-T, the membranes were incubated with the corresponding secondary antibody HRP-conjugated goat anti-mouse or rabbit immunoglobulin IgG (1:2000 dilution; Abcam, USA). After being incubated for 1 h at 37°C, the protein bands were detected by using a ChemiDoc XRS+ Imaging system (Bio-Rad Laboratories, Inc., USA), and the protein density was quantified with Odyssey v1.2 software (LI-COR Biosciences, NE, USA).

MTT Cell Proliferation Assay

Cell proliferation was estimated by a 3-(4,5-Dimethylthiazol-2-yl)-2,5-diphenyltetrazolium bromide (MTT) assay. Incubated NSCLC cells were harvested and seeded in 96-well plates with 100 μl fresh DMEM medium at a density of 4, 000 cells/well

Table 1. Primer Sequences for RT-qPCR.

Genes	Forward	Reverse
miR-499a-5p	5'-GCCCTGTCCCCTGTGCCTT-3'	5'-AAACATCACTGCAAGTCTT-3'
FGF9	5'-GGCCTGGTCAGCATTCGAG-3'	5'-GTATCGCCTTCCAGTGTCCAC-3'
MRPS35	5'-GGAAAGAACACCCGGAAATGA-3'	5'-GTGCTGCAACTGGGTAAACAC-3'
HNRNPC	5'-CCCTTCTCCGTCCCCTCTAC-3'	5'-CCCGAGCAATAGGAGGAGGA-3'
SRSF4	5'-GCCCTCCTACTCGCACAGA-3'	5'-GCGTCCCTTGTGAGCATCT-3'
PRKAR1A	5'-CACTGCTCGACCTGAGAGAC-3'	5'-CCGCATCTTCCTCCGTGTAG-3'
U6	5'-CTCGCTTCGGCAGCACA-3'	5'-AACGCTTCACGAATTTGC-3'
ACTB	5'-CATGTACGTTGCTATCCAGGC-3'	5'CTCCTTAATGTCACGCACGAT-3'

RT-qPCR, reverse transcription quantitative real-time; FGF9, fibroblast growth factor 9; MRPS35, mitochondrial ribosomal protein S35; HNRNPC, heterogeneous nuclear ribonucleoprotein C; SRSF4, serine and arginine rich splicing factor 4; PRKAR1A, protein kinase cAMP-dependent type I regulatory subunit alpha; U6, U6 small nuclear RNA; ACTB, actin beta.

the day prior to transfection, and then transfected with these oligonucleotides by using Lipofectamine 2000. 20 μL MTT solution (5 mg/ml, Sigma-Aldrich, MO, USA) was added into each well once a day for days. After 4 h incubation, the original culture solution was discarded and 150 μl dimethyl sulfoxide (DMSO) was added to dissolve the excessive crystals. Optical absorbance of cells was measured using a multifunctional microplate reader (Bio-Rad, Hercules, CA, USA) at 490 nm.

Colony Formation Assay

Cells were trypsinized to single cell suspensions 24 h after transfection with with these oligonucleotides by using Lipofectamine 2000. Then, the NSCLC cells were seeded into fresh 6-well plates at 600 cells/well. After 2 weeks, the colonies were fixed with absolute methanol for 1 h at 37°C, and then stained with crystal violet for 10 min at 37°C. The colonies with a diameter over 2 mm were counted by a ECLIPSE TS100 light microscope (Nikon Corporation, Tokyo, Japan).

In Vivo Tumorigenicity Assay

Animal experiments were approved by the Animal Care and Use Committee of Tianjin First Central Hospital (permit number: TJ201601071). Four-week-old male BALB/c nude mice were purchased from the Institute of Model Animals of Nanjing University (Nanjing, China). All mice were housed and kept in a specific pathogen-free (SPF) suite, and were randomly divided into 2 groups and injected subcutaneously with H1299 cells (3×10^6 cells/mouse in 0.2 ml of PBS, n = 20) that were stably transfected with agomiR-499a-5p or agomiR-NC. Tumor growth curve was monitored, and tumor volume was calculated according to the formula: $a \times b^2 \times \pi/6$, where a is the longest diameter and b is the shortest diameter. All mice were anesthetized with intraperitoneal injection of sodium pentobarbital (35 mg/kg) and then sacrificed by cervical dislocation after 4 weeks, and then the tumors were collected and weighed.

RNA Isolation and Reverse Transcription Quantitative Real-Time (RT-qPCR) Analysis

Total RNA was extracted from tissues and cell lines using TRIzol® reagent (Invitrogen, CA, USA), and quantified using a NanoDrop spectrophotometer (Thermo Scientific, Rockford, IL, USA). The miRNA cDNA Synthesis Kit (Invitrogen, CA, USA) was applied for cDNA generation of miR-499a-5p, according to the manufacturers' protocols. Simultaneously, the mRNA was reversely transcribed into cDNA by using a PrimeScript RT Reagent Kit (Takara, Dalian, China). The quantitative analysis was assayed using a MiScript SYBR Green PCR Kit on an Applied Biosystems 7900HT Fast Real-Time PCR System (Applied Biosystems, Foster City, CA, USA). The primers of miR-499a-5p, FGF9, mitochondrial ribosomal protein S35 (MRPS35), heterogeneous nuclear ribonucleoprotein C (HNRNPC), serine and arginine rich splicing factor 4 (SRSF4), protein kinase cAMP-dependent type I regulatory subunit alpha (PRKAR1A), U6 small nuclear RNA (U6) and ACTB (actin beta) were shown in Table 1. U6 and ACTB were used as internal controls for the miR-499a-5p and other protein coding genes, respectively. The fold changes of genes were calculated through relative quantification using the $2^{-\Delta\Delta Ct}$ method.[19]

Cell Cycle Assay

NSCLC cells were rinsed thrice with cold PBS. Then, cells were collected and cell concentration were adjusted to 1×10^6/ml. 1 ml of single cell suspension were taken to perform cell cycle assay. After removing the supernatant, cells were fixed in cold 75% ethanol overnight at 4°C. After 3 rinses with cold PBS, cells were treated with RNase A in a 37°C thermostat water bath for 30 min and stained with PI (Sigma-Aldrich, MO, USA) in the dark at 4°C for 20 min. Subsequently, cells were detected by using FACSCalibur flow cytometer (BD Biosciences, San Jose, CA, USA). All experiments were carried out in triplicate with separate cultures and the data were analyzed with a FlowJo software (FlowJo, Ashland, OR, USA).
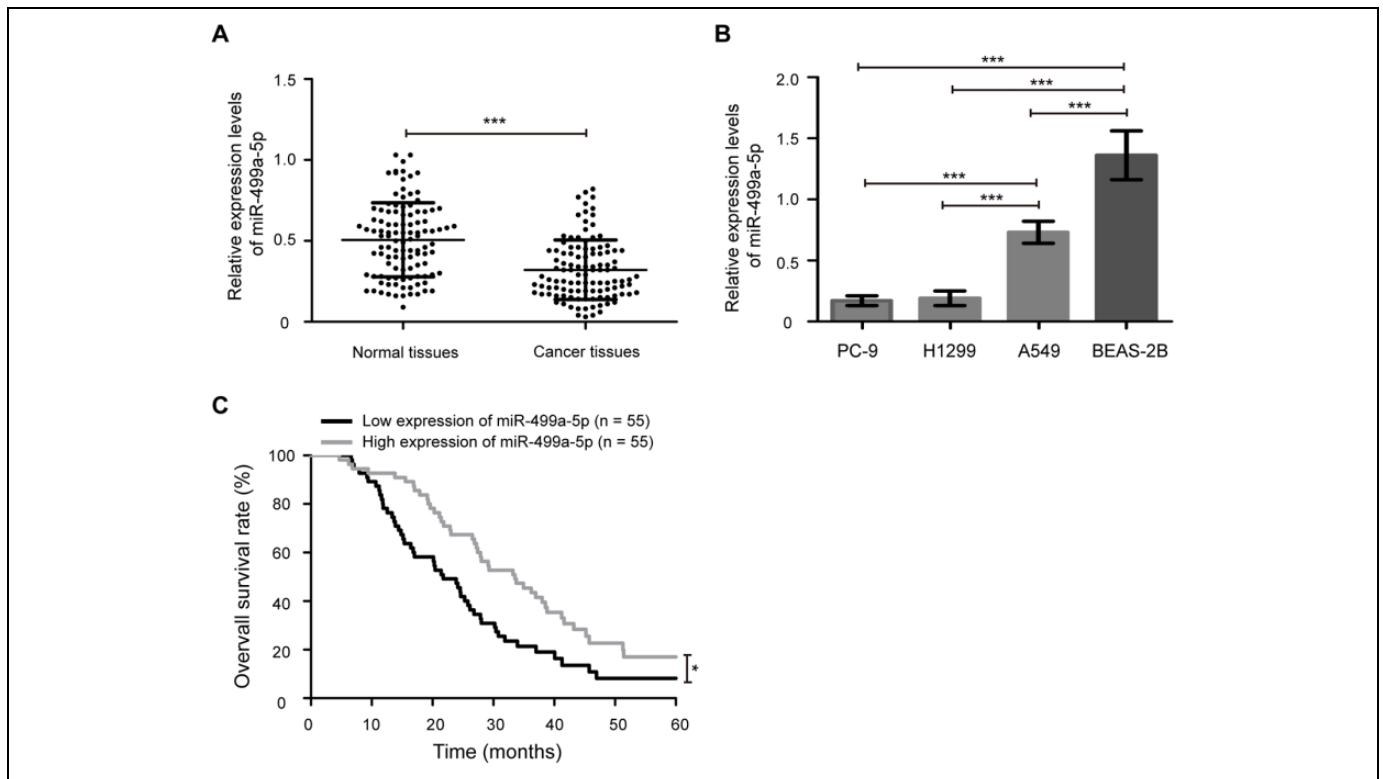
Figure 1. Expression pattern of miR-499a-5p in NSCLC samples and cell lines. (A) Reverse transcription quantitative real-time (RT-qPCR) analysis of miR-499a-5p expression in cancer tissues and matched adjacent normal tissues from 110 cases of NSCLC patients. (B) The expression of miR-499a-5p in NSCLC cell lines A549, H1299, and PC-9, and a human normal epithelial cell line BEAS-2B. (C) NSCLC patients with low expression of miR-499a-5p exhibited worse a overall survival rate compared with those patients with high expression of miR-499a-5p. miR, microRNA. Data presented as the mean $\pm$ standard deviation (SD) of 3 replicates. ***$P < 0.001$.

Target Prediction and Luciferase Report Assay

Bioinformatics analysis was performed using TargetScan (http://www.targetscan.org/), miRBase (http://www.mirbase.org/), and miRDB (http://www.mirdb.org/). The luciferase assay was performed as described previously. Briefly, NSCLC cells were co-transfected with 0.5 μg FGF9 3'-UTR wild type (WT) or mutant (MUT) luciferase reporter plasmid and 50 nM agomiR-499a-5p and agomiR-NC or antagomiR-499a-5p and antagomiR-NC. Luciferase activities were detected 48 h post-transfection using a dual-luciferase reporter assay system (Promega, Madison, WI, USA) and a GloMax-Multi Jr Single Tube Multimode Reader (Promega, Madison, WI, USA). The luciferase activities of firefly were normalized against Renilla to represent the relative luciferase activity of cells with different transfection.

Statistical Analysis

Statistical analysis was conducted using SPSS 19.0 (SPSS Inc., Chicago, IL, USA). All measurement data were expressed as mean $\pm$ standard deviation (SD) of results from at least 3 independent experiments. Chi-square (χ^2) test was applied to determine the association between the miR-499a-5p expression and the clinicopathological features of NSCLC patients. The association between miR-499a-5p expression and the overall

survival of NSCLC patients was analyzed by Kaplan-Meier method and log-rank test. The correlation between miR-499a-5p and FGF9 expression in tumor specimens and were determined by Spearman's correlation analysis. Comparisons between groups was performed using Student's paired t-test or 1-way analysis of variance followed by Bonferroni post-test. Difference was considered as significant if the P value was less than 0.05.

Results

The Expression and Clinical Significance of miR-499a-5p in NSCLC

To investigate the potential roles of miR-499a-5p in NSCLC development, we first determined its expression in NSCLC samples and cell lines. As shown in Figure 1A, the expression levels of miR-499a-5p were significantly downregulated in cancer tissues compared with matched adjacent normal tissues ($P < 0.001$). Similarly, decreased miR-499a-5p expression was also observed in 3 NSCLC cell lines (A549, H1299, and PC-9) compared with human normal bronchial epithelial cell line BEAS-2B (Figure 1B, $P < 0.001$). In addition, the expression of miR-499a-5p was lower in H1299 and PC-9 cell lines than that in A549 cell line ($P < 0.001$). Therefore, H1299 and PC-9

Table 2. Association Between miR-499a-5p Expression and Clinicopathological Characteristics of Patients With NSCLC Patients.

Clinicopathological characteristics	Cases (n)	miR-499a-5p		P value
		Low (n, %)	High (n, %)	
Age (years)				0.695
< 55	42	22 (20.0)	20 (18.2)	
≥ 55	68	33 (30.0)	35 (31.8)	
Gender				0.177
Male	63	28 (25.5)	35 (31.8)	
Female	47	27 (24.5)	20 (18.2)	
Tumor size (cm)				< 0.001
< 3	76	29 (26.4)	47 (42.7)	
≥ 3	34	26 (23.6)	8 (7.3)	
Differentiation				0.056
Well/moderate	50	20 (18.2)	30 (27.3)	
Poor	60	35 (31.8)	25 (22.7)	
Histological type				0.305
Adenocarcinoma	29	11 (10.0)	18 (16.4)	
Squamous cell carcinoma	43	24 (21.8)	19 (17.3)	
Others	38	20 (18.2)	18 (16.4)	
TNM stage				0.001
I/II	69	26 (23.6)	43 (39.1)	
III	41	29 (26.4)	12 (10.9)	
Lymph node metastasis				0.101
No	87	40 (36.4)	47 (42.7)	
Yes	23	15 (13.6)	8 (7.3)	
Smoking				0.152
No	75	34 (30.9)	41 (37.3)	
Yes	35	21 (19.1)	14 (12.7)	

cell lines were selected for overexpression experiments and A549 cell line was chose for knockdown experiments.

According to the median level of miR-499a-5p in cancer tissues, NSCLC patients were divided in to low (n = 55) and high (n = 55) expression groups. As shown in **Table 2**, decreased miR-499a-5p expression was associated with larger tumor size ($P < 0.001$) and higher TNM stage ($P = 0.001$). Nevertheless, miR-499a-5p expression was not associated with other clinicopathological characteristics, including age ($P = 0.695$), gender ($P = 0.177$), smoking ($P = 0.152$), histological type ($P = 0.305$), differentiation ($P = 0.056$), and lymph node metastasis ($P = 0.101$). Furthermore, to evaluate the correlation between the expression of miR-499a-5p and prognosis in NSCLC patients, the Kaplan-Meier analysis and log-rank test were used. It could be seen from Figure 1C that NSCLC patients with low expression of miR-499a-5p exhibited a worse overall survival rate compared with those patients with high expression of miR-499a-5p ($P < 0.05$). These results suggest that downregulated expression of miR-499a-5p predicts a poor overall survival in patients with NSCLC.

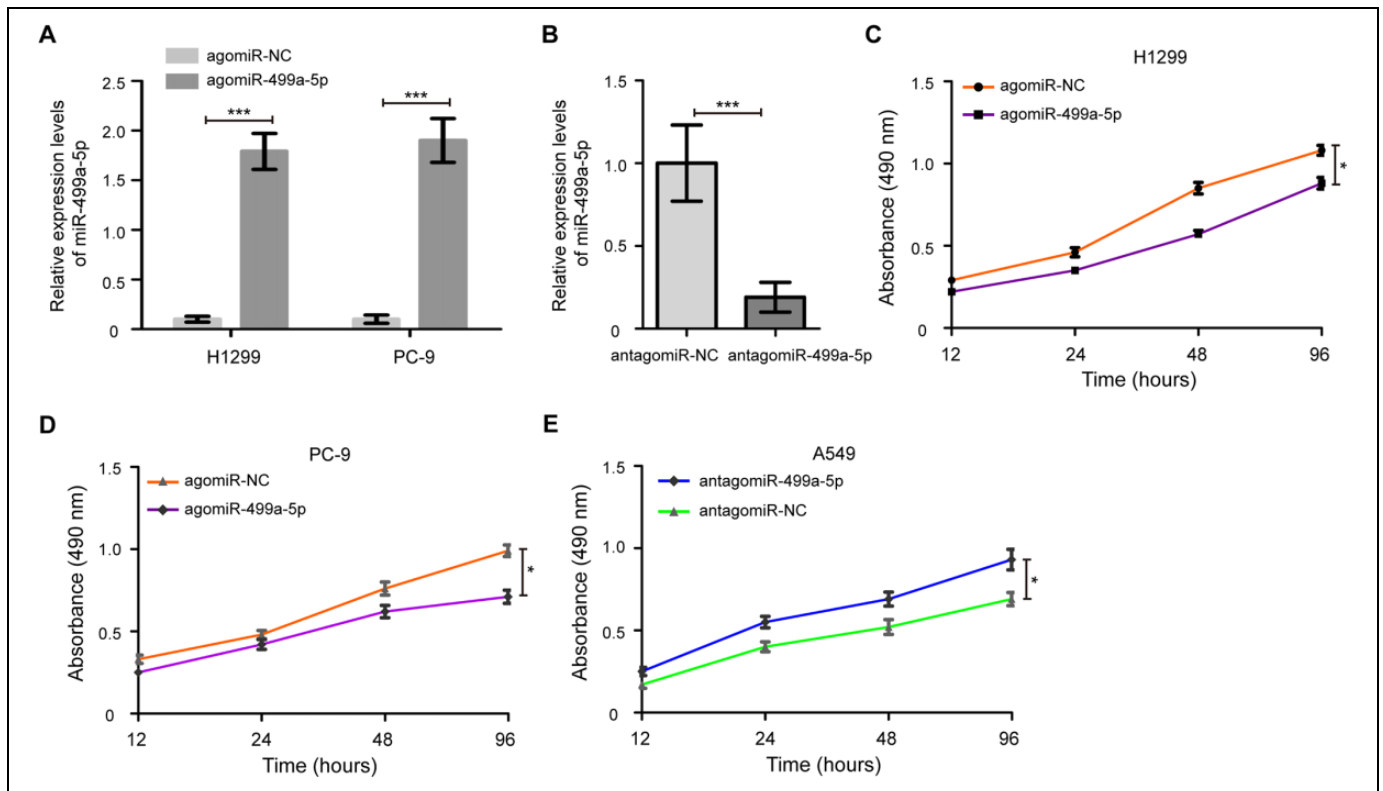## miR-499a-5p Suppresses NSCLC Cells Proliferation In Vitro

To improve the understanding of the effect of miR-499a-5p on cell proliferation, H1299 and PC-9 cells were treated with the agomiR-499a-5p and agomiR-NC. As shown in Figure 2A, transfection of the agomiR-499a-5p led to a dramatic increase in miR-499a-5p expression in H1299 and PC-9 cells ($P < 0.001$). Meanwhile, after transfection of antagomiR-499a-5p, we found that the miR-499a-5p expression was remarkably decreased in A549 cells (Figure 2B, $P < 0.001$). Importantly, enhanced expression of miR-499a-5p significantly inhibited cell proliferation of H1299 and PC-9 cells compared with the agomiR-NC treated cells (Figure 2C and D, $P < 0.05$). Furthermore, A549 cells with the antagomiR-499a-5p had a higher cell proliferation than the cells treated with antagomiR-NC (Figure 2E, $P < 0.05$). In addition, colony formation assays revealed that the agomiR-499a-5p significantly decreased the growth of H1299 and PC-9 cells compared to agomiR-NC-transfected cells, while antagomiR-499a-5p remarkably increased the growth of A549 cells compared to antagomiR-NC-transfected cells (Figure S1, $P < 0.05$).

To further explore the potential mechanism underlying the inhibitory effect on cell proliferation by overexpression of miR-499a-5p, cell cycle analysis was performed. Upon overexpression of miR-499a-5p, the percentages of H1299 and PC-9 cells in G0/G1 phase clearly increased compared with the agomiR-NC groups (Figure 3A, $P < 0.05$). Compared with the antagomiR-NC group, the S phase was obviously increased in A549 cells transfected with the antagomiR-499a-5p (Figure 3B, $P < 0.05$). Meanwhile, after transfection of agomiR-499a-5p and antagomiR-499a-5p, we found that the protein expression levels of CCND1 were remarkably decreased and increased in NSCLC cells, respectively (Figure 3C and D, $P < 0.001$). Collectively, these results suggest that miR-499a-5p suppresses NSCLC cells proliferation by hampering the G0/G1- to S-phase cell cycle transition.

miR-499a-5p Restrains the Tumorigenesis of NSCLC In Vivo

To examine the roles of miR-499a-5p in tumor formation *in vivo*, a nude mouse xenograft model was performed. The H1299 cells with agomiR-499a-5p and agomiR-NC were subcutaneously inoculated into BALB/c nude mice, and tumor volumes were measured and xenografts were weighed. As shown in Figure 3A, tumors derived from agomiR-499a-5p transfected cells grew more slowly in comparison with the agomiR-NC treated cells (Figure 4A, $P < 0.01$). Moreover, the final tumor volumes (Figure 4B, $P < 0.001$) of the agomiR-499a-5p group were significantly lower than that of the agomiR-NC group. The average weight of tumor in the agomiR-499a-5p group was significantly reduced compared with the agomiR-NC group (Figure 4C, $P < 0.001$). In addition, the expression levels of miR-499a-5p in tumor tissues from the agomiR-499a-5p group were markedly increased, compared with the agomiR-NC group, as illustrated by RT-qPCR assay (Figure 4D, $P < 0.001$). These results demonstrate that miR-499a-5p inhibits the tumorigenesis of NSCLC.

Figure 2. miR-499a-5p suppresses NSCLC cell proliferation. (A) Relative expression levels of miR-499a-5p following transfection with agomiR-499a-5p and agomiR-NC in H1299 and PC-9 cells. (B) miR-499a-5p expression was detected in A549 cells after transfection of antagomiR-499a-5p and antagomiR-NC. (C) Cell proliferation capacity was significantly reduced in the miR-499a-5p-expressing H1299 cells, as determined by a MTT assay. (D) Cell growth was also observed to be decreased in the agomiR-499a-5p transfected PC-9 cells compared with the agomiR-NC treated cells. (E) Knockdown of miR-499a-5p promoted A549 cells proliferation. NC, negative control; MTT, 3-(4,5-Dimethylthiazol-2-yl)-2,5-diphenyltetrazolium bromide. Data were presented as the mean values $\pm$ SD from triplicate experiments. $*P < 0.05$, $***P < 0.001$.

FGF9 Is a Direct Target Gene of miR-499a-5p

To further examine the mechanisms underlying miR-499a-5p-mediated suppression of NSCLC tumorigenesis, we employed 3 computational algorithms to predict potential target genes of miR-499a-5p. Five genes (FGF9, MRPS35, NRNPC, SRSF4, PRKAR1A) was found, and the FGF9 expression was downregulated and upregulated the most by overexpression and knockdown of miR-499a-5p in H1299 and A549 cells, respectively (Figure S2, $P < 0.05$). Moreover, FGF9 mRNA expression was significantly higher in cancer tissues compared with matched adjacent normal tissues (Figure S3A, $P < 0.001$). Spearman's correlation analysis showed a significant inverse correlation between FGF9 mRNA level and miR-499a-5p expression in NSCLC samples (Figure S3B, $P < 0.001$). So FGF9 had been chose for further experiment.

As shown in Figure 5A, a complimentary binding region for miR-499a-5p was found in the 3'-UTR of FGF9 mRNA. To further confirm our finding that miR-499a-5p could directly targeting FGF9 expression, a luciferase report assay was performed. As shown in Figure 5B, co-transfection of H1299 cells with FGF9 3'-UTR WT luciferase reporter plasmid and the

agomiR-499a-5p caused a significant reduction in the relative luciferase activity compared with that of the agomiR-NC group ($P < 0.001$). By contrast, FGF9 3'-UTR MUT luciferase reporter plasmid had no significant effect on the relative luciferase activity in the agomiR-499a-5p transfected H1299 cells, compared with that in the agomiR-NC transfected cells. Conversely, miR-499a-5p knockdown substantially escalated the relative luciferase activity of the luciferase reporter plasmid in A549 cells that carried the FGF9 3'-UTR WT but not FGF9 3'-UTR MUT (Figure 5C, $P < 0.001$). Besides, we quantified the expression of FGF9 protein in H1299 cells transected with the agomiR-499a-5p by Western blot analysis. The results indicated that the protein expression of FGF9 was obviously downregulated in H1299 cells that were transfected with the agomiR-499a-5p (Figure 5D, $P < 0.001$). Meanwhile, FGF9 protein expression was remarkably increased in A549 cells by miR-499a-5p knockdown (Figure 5E, $P < 0.001$). Consistent with the *in vitro* studies, the protein levels of FGF9 in tumor tissues from mice in the agomiR-499a-5p group were markedly reduced compared with the agomiR-NC group (Figure 5F, $P < 0.001$). Together, these results suggest that FGF9 is a direct target gene of miR-499a-5p.
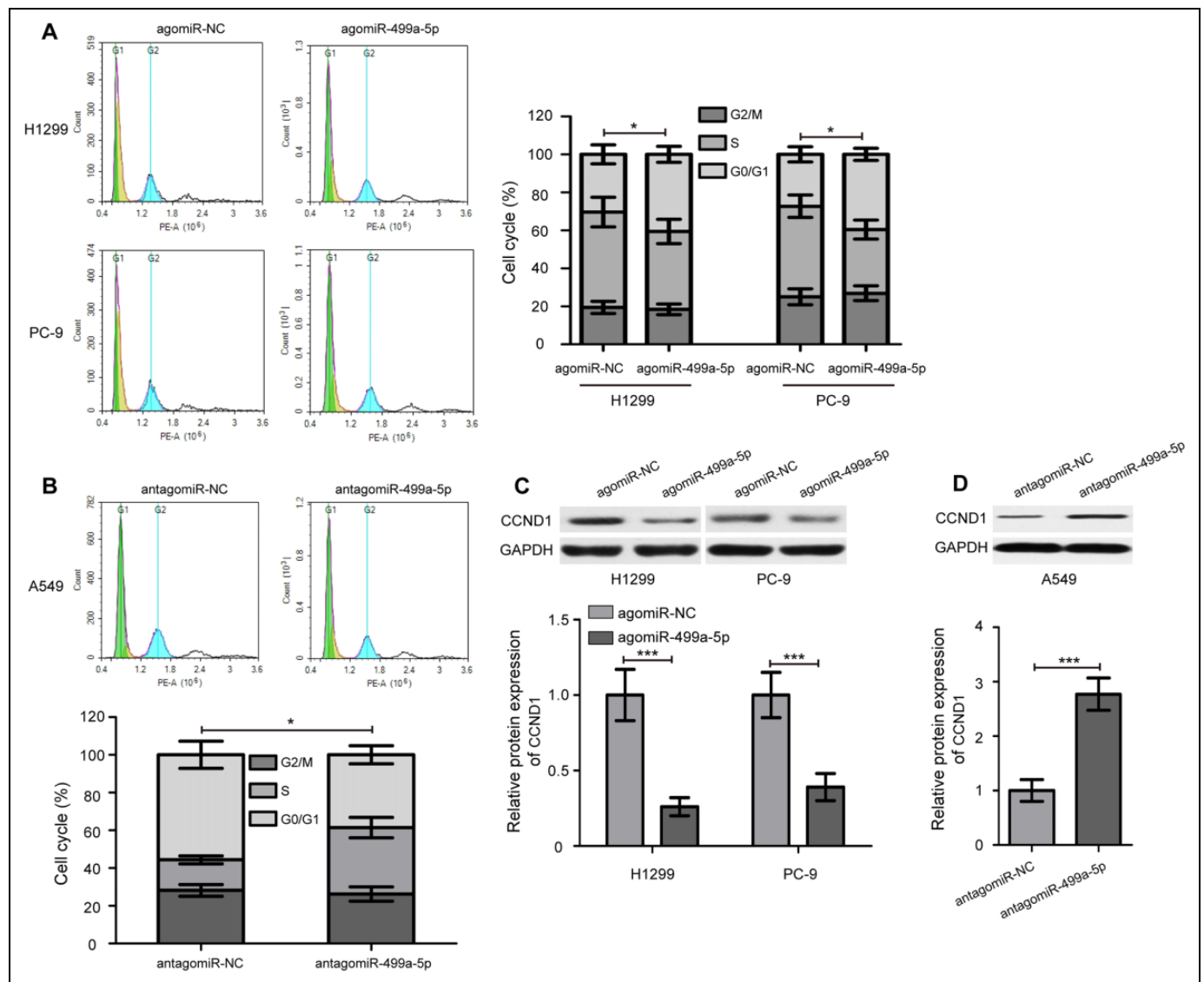
Figure 3. miR-499a-5p hampers the G0/G1- to S-phase cell cycle transition. (A) miR-499a-5p induced cell cycle arrest at G0/G1 phase in H1299 and PC-9 cells. (B) Knockdown of miR-499a-5p increased the S phase of A549 cells. (C) Western blot analysis of CCND1 protein expression in H1299 and PC-9 cells after transfection of agomiR-499a-5p and agomiR-NC. (D) Knockdown of miR-499a-5p remarkably increased CCND1 protein expression in A549 cells. CCND1, cyclin D1. Data presented as the mean $\pm$ SD of 3 replicates. *P < 0.05, ***P < 0.001.

Silencing of FGF9 Partly Abrogates miR-499a-5p Knockdown-Induced Promotive Effect on NSCLC Cell Proliferation

Due to the negatively regulation of miR-499a-5p on FGF9 in NSCLC cells, we speculated that the role of miR-499a-5p in regulating NSCLC cells proliferation was mediated by targeting FGF9 expression. We transfected siFGF9 and siCtrl into the antagomiR-499a-5p treated A549 cells, and functional rescue experiments were performed. The results revealed that siFGF9 could decrease the protein expression of FGF9 in A549 cells treated with antagomiR-499a-5p (Figure 6A, P < 0.001). More-over, we found that antagomiR-499a-5p knockdown mediated

promotive effect on A549 cell proliferation were partially reversed by co-transfection with antagomiR-499a-5p and siFGF9 (Figure 6B, P < 0.05). Similarly, upregulation of CCND1 protein expression in A549 cells caused by miR-499a-5p knockdown were partially reversed by siFGF9 (Figure 6C, P < 0.001). Collectively, our results demonstrate that downregulation of miR-499a-5p restrains the tumorigenesis of NSCLC by targeting FGF9.

Discussion

Nowadays, with the aggravation of air pollution, deterioration of environment, and prevalence of smoking, NSCLC gradually
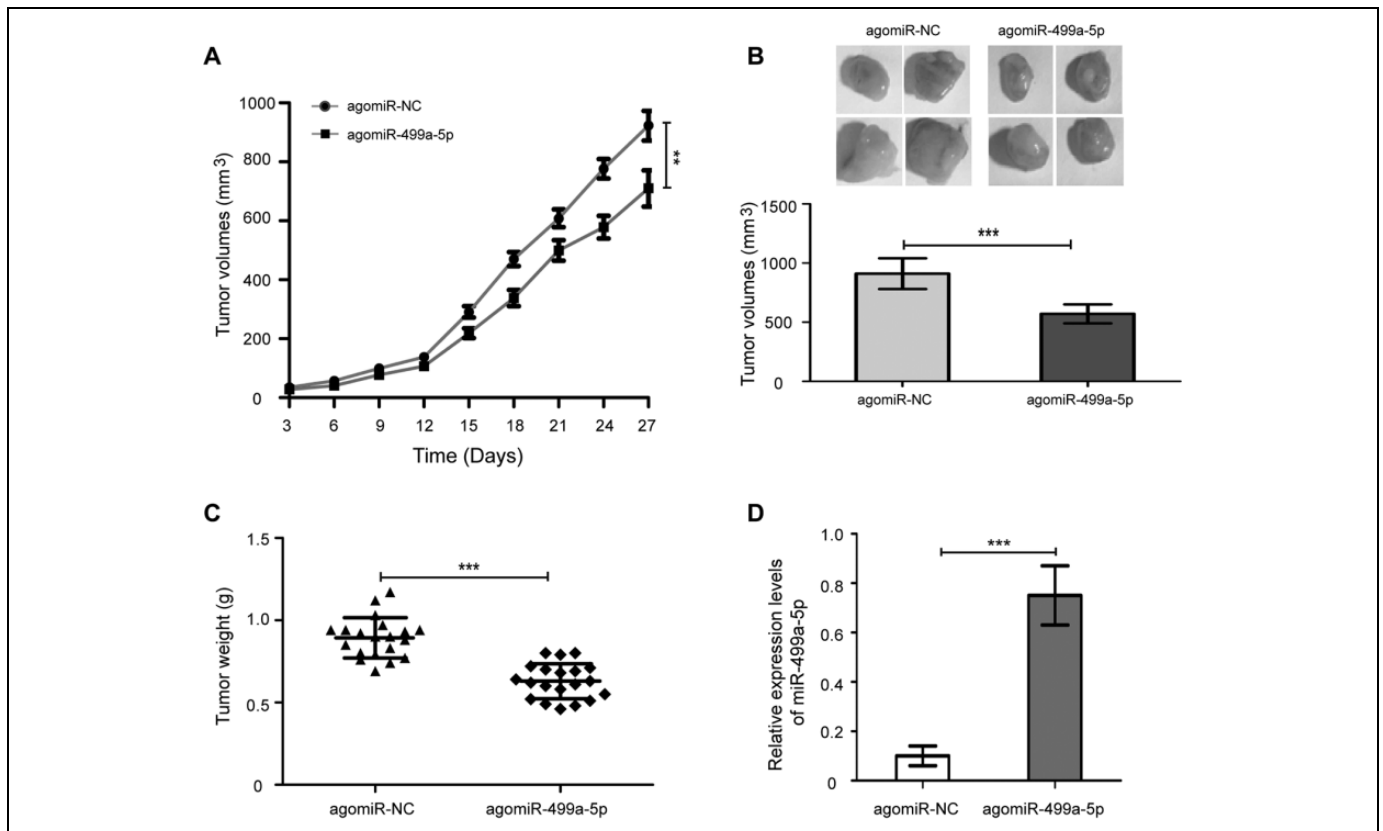
Figure 4. miR-499a-5p restrains the tumorigenesis of NSCLC in a nude mouse xenograft model. (A) Growth of xenograft tumors from miR-499a-5p-expressing H1299 cells was significantly slower than the agomiR-NC treated cells. (B) Measurement of the final volume of xengraft model at 4 weeks. (C) The weight of xenograft tumors derived from miR-499a-5p-expressing H1299 cells was significantly lighter than the control group. (C) RT-qPCR analysis of miR-499a-5p expression in xenograft tumors from individual mice. Values were mean $\pm$ SD. ***P <* 0.01, ****P <* 0.001.

become the most frequent cause of cancer-related deaths globally. Tumorigenesis of NSCLC is a complex and multi-stage process involving the regulation of a wide range of oncogenes and tumor-suppressing genes.[20,21] Among these tumor oncogenic and suppressive genes, miRNA has been recognized to exert regulator roles in epigenetic changes.[22] Dysregulated miRNA takes part in the initiation, progression, and metastasis of multiple human cancers.[23] Among them, miR-499a-5p, has been shown to play a key role in cardiomyogenic differentiation of bone marrow-derived mesenchymal stem cells and has inhibitory effects on the proliferation and differentiation of osteosarcoma.[24,25] However, there is currently no data regarding the functions of miR-499a-5p in NSCLC. In this study, we evaluated the role of miR-499a-5p in the tumorigenesis of NSCLC, as well as the underlying molecular mechanisms.

The present study revealed that the levels of miR-499a-5p were downregulated in cancer tissues in comparison with matched adjacent normal tissues. In addition, we also observed the expression of miR-499a-5p was markedly lower in NSCLC cells than that in BEAS-2B cell line. NSCLC patients with low expression of miR-499a-5p exhibited a worse overall survival rate compared with those patients with high expression

of miR-499a-5p. These findings indicated that miR-499a-5p may play an important role in the modulation of NSCLC development. To better understand the underlying roles of miR-499a-5p in NSCLC, we explored the biological effects of miR-499a-5p on cell proliferation *in vitro and in vivo*. The results showed that miR-499a-5p suppressed NSCLC cell proliferation by hampering the G0/G1- to S-phase cell cycle transition. Moreover, restoration of miR-499a-5p restrained NSCLC tumorigenesis in a nude mouse xenograft model. These results were consistent with previous finding on the antiproliferative activity of miR-499a-5p.[25] Similarly, the inhibitory roles of various miRNAs in tumorigenesis of NSCLC have been reported in previous studies. Meng et al showed that miR-377 plays an important role in the tumorigenesis of NSCLC by targeting astrocyte elevated gene-1, and may be a potential therapeutic target for lung cancer.[26] Xu et al suggested that miR-30e-5p suppresses NSCLC tumorigenesis by targeting ubiquitin carboxyl-terminal hydrolase 22-mediated Sirt1/JAK/STAT3 signaling.[27] Zhang et al demonstrated that miR-300 targets hypoxia inducible factor-3 alpha to inhibit tumorigenesis of NSCLC.[28] Thus, downregulation of miR-499a-5p restrains the tumorigenesis of NSCLC and represents a potential target for NSCLC treatment.
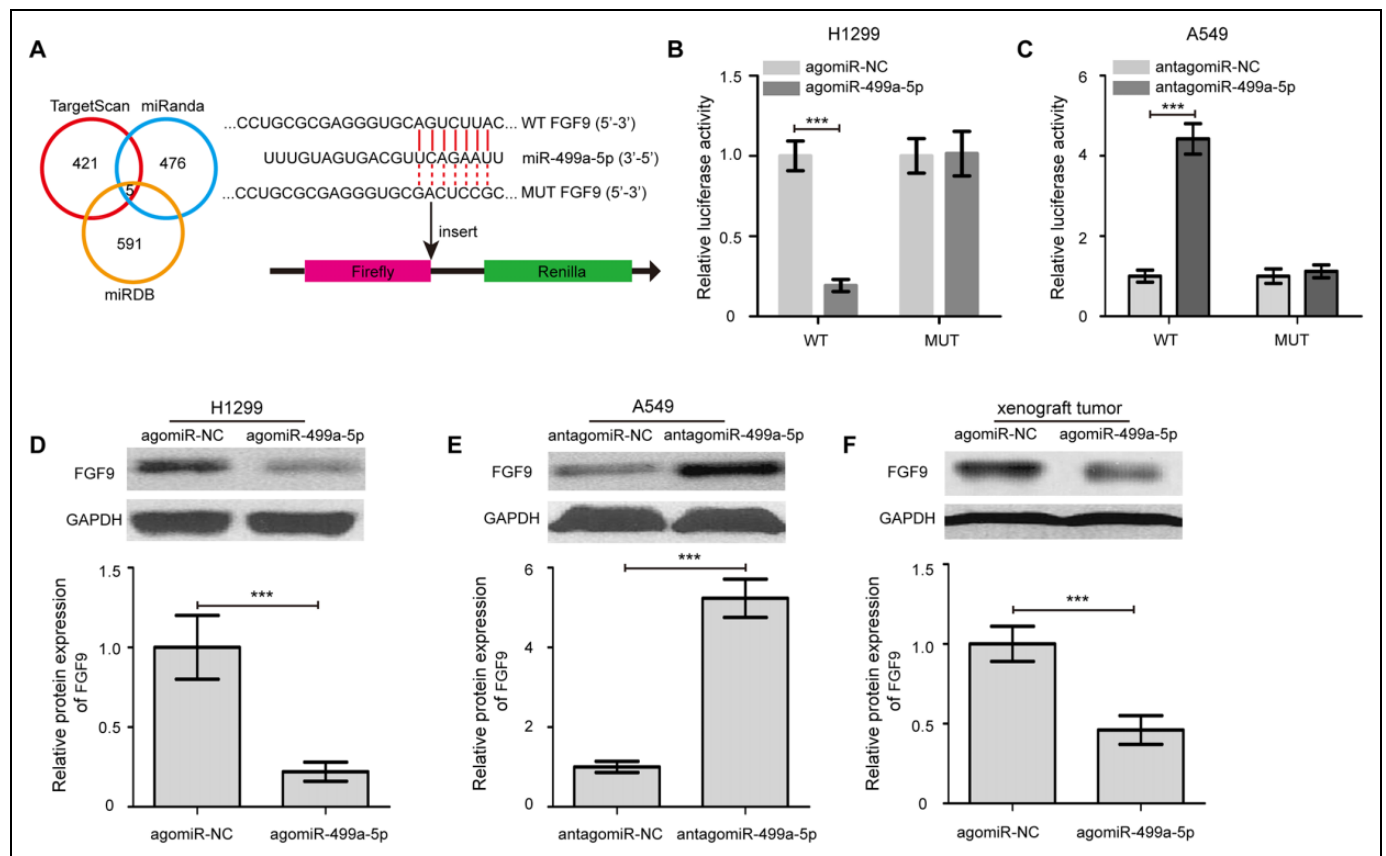
Figure 5. FGF9 is a direct target gene of miR-499a-5p. (A) FGF9 was identified as a potential target gene of miR-499a-5p by using 3 computational algorithms. (B) The relative luciferase activity was normalized to the Renilla luciferase activity after co-transfection of cells with the agomiR-499a-5p or agomiR-NC and FGF9 3′-UTR wild type (WT) or mutant (MUT) luciferase reporter plasmid in H1299 cells. (C) Luciferase activities were measured in A549 cells following cotransfection with the FGF9 3′-UTR WT or MUT reporter plasmids and antagomiR-499a-5p or antagomiR-NC. (D) Transfection of the agomiR-499a-5p markedly decreased FGF9 protein expression in H1299 cells in compared with the agomiR-NC treated cells. (E) FGF9 protein expression was remarkably increased in A549 cells by miR-499a-5p knockdown. (F) The protein level of FGF9 in tumor tissues from mice in the agomiR-499a-5p group was markedly reduced compared with the agomiR-NC group. Data were presented as the mean values $\pm$ SD from triplicate experiments. FGF9, fibroblast growth factor 9. ***$P < 0.001$.

We further studied the mechanisms underlying the miR-499a-5p-mediated antiproliferative activity in NSCLC. Our bioinformatics analysis revealed that there were 5 of possible target genes of miR-499a-5p, among which FGF9 was selected for further study. FGF9 belongs to the FGF family that participates in a spectrum of biological processes including tumor growth.[29] Several studies have suggested that FGF9 has been implicated in the etiology and pathogenesis of many human cancers, including prostate, endometrioid, and lung cancer.[16-18] FGF9 was proved to be targeted by miRNAs, such as miR-214 in gastric cancer and miR-187 cervical cancer.[30,31] In this study, we identified that FGF9 was a direct target of miR-499a-5p in NSCLC. Our results testified that the protein expression of FGF9 was significantly decreased and increased in NSCLC cells by miR-499a-5p overexpression and knockdown, respectively. Moreover, luciferase reporter assay unmasked the binding sites between miR-499a-5p and FGF9 3′-UTR in favor of the forceful suppression effect of miR-499a-5p on FGF9

expression. Therefore, FGF9 is a direct target gene of miR-499a-5p.

These above data encouraged us to hypothesize that miR-499a-5p might exert its suppressive functions by targeting FGF9. In support of this hypothesis, reduced FGF9 expression by siFGF9 was noted in antagomiR-499a-5p inhibitor treated A549 cells. Rescue experiments provided the evidences that antagomiR-499a-5p treated A549 cells transfected with the siFGF9 exhibited significantly lower cell proliferation and reduced CCND1 protein expression. These data demonstrated that downregulation of miR-499a-5p restrains the tumorigenesis of NSCLC by targeting FGF9.

In summary, we observe the downregulation of miR-499a-5p in NSCLC, and demonstrate that miR-499a-5p predicts a worse prognosis and restrains the tumorigenesis of NSCLC by targeting FGF9. These findings suggest that miR-499a-5p/FGF9 axis may serve as a potential therapeutic candidate in the developing novel strategy for NSCLC treatment.
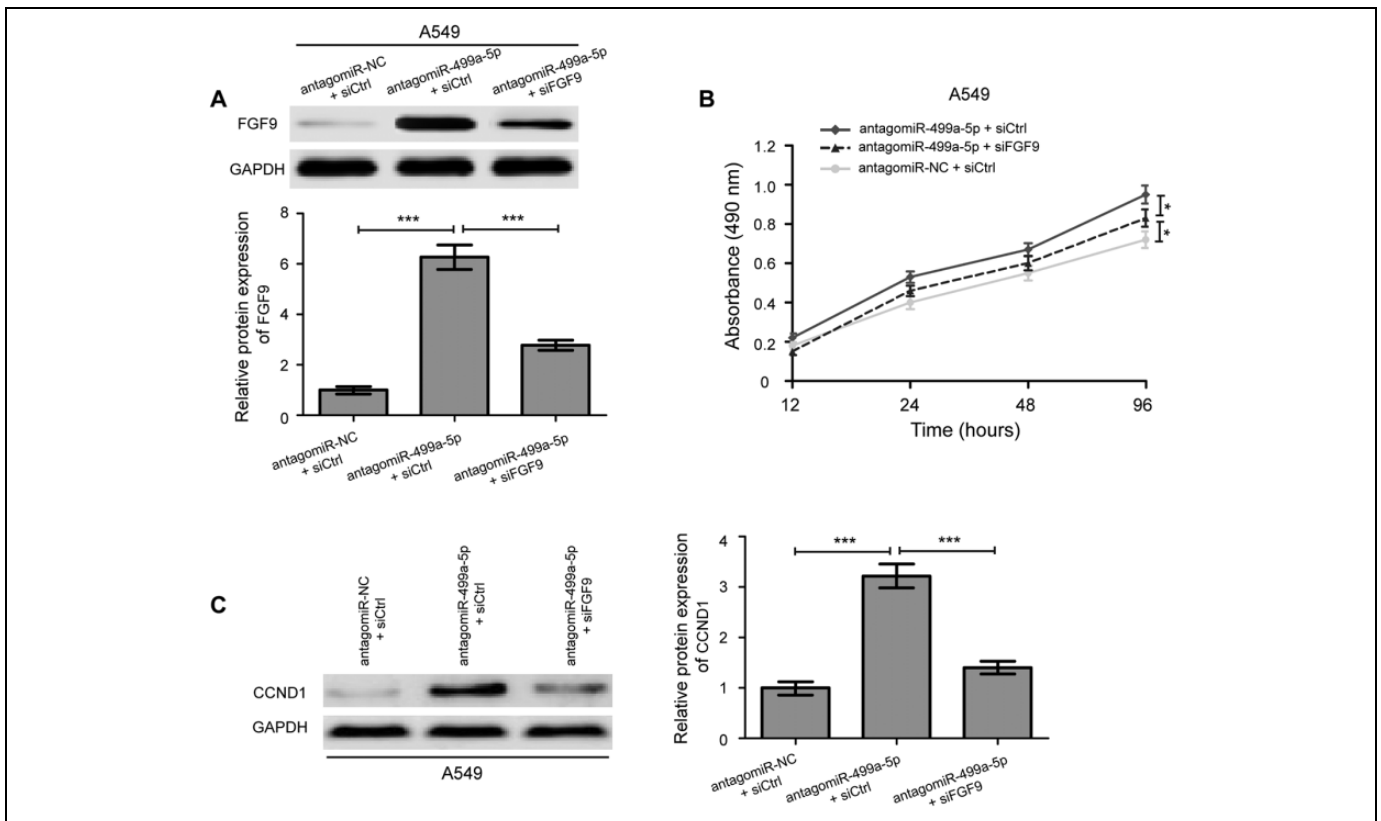
Figure 6. Silencing of FGF9 partly abrogates miR-499a-5p knockdown-induced promotive effect on NSCLC cells growth. (A) Western blotting analysis of FGF9 expression in antagomiR-499a-5p treated A549 cells after transfected with either siFGF9 or siCtrl. (B) FGF9 knockdown reversed the growth-suppressive effect of antagomiR-499a-5p on A549 cells. (C) Western blotting was performed to determine the protein expression levels of CCND1 in antagomiR-499a-5p treated A549 cells after transfected with siFGF9. siFGF9, FGF9 siRNA; siCtrl, control siRNA. Data were presented as the mean $\pm$ SD of 3 replicates. *P < 0.05, ***P < 0.001.

Authors' Note

Declaration of Conflicting Interests

Funding

ORCID iD

Lihong Zhao https://orcid.org/0000-0003-3974-6304

Supplemental Material

Supplemental material for this article is available online.

References

1. Siegel RL, Miller KD, Jemal A. Cancer statistics, 2016. *CA Cancer J Clin*. 2016;66(1):7-30.

2. Nanavaty P, Alvarez MS, Alberts WM. Lung cancer screening: advantages, controversies, and applications. *Cancer Control*. 2014;21(1):9-14.

3. Woodard GA, Jones KD, Jablons DM. Lung cancer staging and prognosis. *Cancer Treat Res*. 2016;170:47-75.

4. Liam CK, Andarini S, Lee P, et al. Lung cancer staging now and in the future. *Respirology*. 2015;20(4):526-534.

5. Skvortsova K, Iovino N, Bogdanovic O. Functions and mechanisms of epigenetic inheritance in animals. *Nat Rev Mol Cell Biol*. 2018;19(12):774-790.

6. Morales S, Monzo M, Navarro A. Epigenetic regulation mechanisms of microRNA expression. *Biomol Concepts*. 2017;8(5-6): 203-212.

7. Hwang HW, Mendell JT. MicroRNAs in cell proliferation, cell death, and tumorigenesis. *Br J Cancer*. 2006;94(6):776-780.

8. Mo YY. MicroRNA regulatory networks and human disease. *Cell Mol Life Sci*. 2012;69(21):3529-3531.

9. Lu J, Zhan Y, Feng J, et al. MicroRNAs associated with therapy of non-small cell lung cancer. *Int J Biol Sci*. 2018;14(4):390-397.

10. Hu WB, Wang L, Huang XR, Li F. MicroRNA-204 targets SOX4 to inhibit metastasis of lung adenocarcinoma. *Eur Rev Med Pharmacol Sci*. 2019;23(4):1553-1562.

11. An Y, Zhang Q, Li X, Wang Z, Li Y, Tang X. Upregulated microRNA miR-21 promotes the progression of lung adenocarcinoma through inhibition of KIBRA and the Hippo signaling pathway. *Biomed Pharmacother*. 2018;108:1845-1855.

12. Li T, Wang X, Jing L, Li Y. MiR-1-3p inhibits lung adenocarcinoma cell tumorigenesis via targeting protein regulator of cytokinesis 1. *Front Oncol*. 2019;9:120.

13. Ren ZP, Hou XB, Tian XD, et al. Identification of nine microRNAs as potential biomarkers for lung adenocarcinoma. *FEBS Open Bio*. 2019;9(2):315-327.

14. Zhan JW, Jiao DM, Wang Y, et al. Integrated microRNA and gene expression profiling reveals the crucial miRNAs in curcumin anti-lung cancer cell invasion. *Thorac Cancer*. 2017;8(5): 461-470.

15. Corn PG, Wang F, McKeehan WL, Navone N. Targeting fibroblast growth factor pathways in prostate cancer. *Clin Cancer Res*. 2013;19(21):5856-5866.

16. Yang H, Fang F, Chang R, Yang L. MicroRNA-140-5p suppresses tumor growth and metastasis by targeting transforming growth factor beta receptor 1 and fibroblast growth factor 9 in hepatocellular carcinoma. *Hepatology*. 2013;58(1):205-217.

17. Rao C, Miao X, Zhao G, et al. MiR-219a-5p enhances cisplatin sensitivity of human non-small cell lung cancer by targeting FGF9. *Biomed Pharmacother*. 2019;114:108662.

18. Wang Q, Liu S, Zhao X, Wang Y, Tian D, Jiang W. MiR-372-3p promotes cell growth and metastasis by targeting FGF9 in lung squamous cell carcinoma. *Cancer Med*. 2017;6(6):1323-1330.

19. Schmittgen TD, Livak KJ. Analyzing real-time PCR data by the comparative C(T) method. *Nat Protoc*. 2008;3(6):1101-1108.

20. Duruisseaux M, Esteller M. Lung cancer epigenetics: from knowledge to applications. *Semin Cancer Biol*. 2018;51:116-128.

21. Kalainayakan SP, FitzGerald KE, Konduri PC, Vidal C, Zhang L. Essential roles of mitochondrial and heme function in lung cancer bioenergetics and tumorigenesis. *Cell Biosci*. 2018;8:56.

22. Zhang B, Pan X, Cobb GP, Anderson TA. microRNAs as oncogenes and tumor suppressors. *Dev Biol*. 2007;302(1):1-12.

23. Ruan K, Fang X, Ouyang G. MicroRNAs: novel regulators in the hallmarks of human cancer. *Cancer Lett*. 2009;285(2):116-126.

24. Neshati V, Mollazadeh S, Fazly Bazzaz BS, et al. MicroRNA-499a-5p promotes differentiation of human bone marrow-derived mesenchymal stem cells to cardiomyocytes. *Appl Biochem Biotechnol*. 2018;186(1):245-255.

25. Liu J, Huang L, Su P, et al. MicroRNA-499a-5p inhibits osteosarcoma cell proliferation and differentiation by targeting protein phosphatase 1D through protein kinase B/glycogen synthase kinase 3beta signaling. *Oncol Lett*. 2018;15(4):4113-4120.

26. Meng F, Zhang L, Shao Y, Ma Q, Lv H. MicroRNA-377 inhibits non-small-cell lung cancer through targeting AEG-1. *Int J Clin Exp Pathol*. 2015;8(11):13853-13863.

27. Xu G, Cai J, Wang L, et al. MicroRNA-30e-5p suppresses non-small cell lung cancer tumorigenesis by regulating USP22-mediated Sirt1/JAK/STAT3 signaling. *Exp Cell Res*. 2018;362(2):268-278.

28. Zhang Y, Guo Y, Yang C, et al. MicroRNA-300 targets hypoxia inducible factor-3 alpha to inhibit tumorigenesis of human non-small cell lung cancer. *Neoplasma*. 2017;64(4):554-562.

29. Wang S, Lin H, Zhao T, et al. Expression and purification of an FGF9 fusion protein in E. coli, and the effects of the FGF9 subfamily on human hepatocellular carcinoma cell proliferation and migration. *Appl Microbiol Biotechnol*. 2017;101(21):7823-7835.

30. Wang R, Sun Y, Yu W, et al. Downregulation of miRNA-214 in cancer-associated fibroblasts contributes to migration and invasion of gastric cancer cells through targeting FGF9 and inducing EMT. *J Exp Clin Cancer Res*. 2019;38(1):20.

31. Liang H, Luo R, Chen X, Zhao Y, Tan A. miR-187 inhibits the growth of cervical cancer cells by targeting FGF9. *Oncol Rep*. 2017;38(4):1977-1984.